PROCEEDINGS, 41st Workshop on Geothermal Reservoir Engineering
Stanford University, Stanford, California, February 22-24, 2016
SGP-TR-209

Hydrogeologic Windows and Estimating the Prospectivity of Geothermal Resources

Jeffrey Bielicki[1], David Blackwell[2], Dylan Harp[3], Satish Karra[3], Richard Kelley[3], Shari Kelley[4], Richard Middleton[3], Mark Person[5], Glenn Sutula[1], James Witcher[6]

[1]The Ohio State University, Columbus, OH 43210, [2]Southern Methodist University, Dallas, TX 75275, [3]Los Alamos National Laboratory, Los Alamos, NM 87545, [4]New Mexico Bureau of Geology and Mineral Resources, NM Tech, 801 Leroy Place, Socorro, NM 87801, [5]Department of Earth & Environmental Sciences, NM Tech, 810 Leroy Place, Socorro, NM 87801, [6]Witcher and Associates P. O. Box 3142, Las Cruces, NM 88003

bielicki.2@osu.edu

Keywords: geothermal, play fairway, hydrogeologic window, risk, prospecting, New Mexico

ABSTRACT

In this Geothermal Play Fairways Analysis project we sought to develop new ways to analyze geologic, geochemical, and geophysical data to reduce the risk and increase the prospects of successful geothermal exploration and development. We collected, organized, and analyzed data from southwest New Mexico in the context of an integrated framework that combines the data for various signatures of a geothermal resource into a cohesive analysis of the presence of heat, fluid, and permeability. We incorporated data on structural characteristics (earthquakes, geophysical logs, fault location and age, basement depth), topographic and water table elevations, conservative ion concentrations, and thermal information (heat flow, bottom hole temperature, discharge temperature, and basement heat generation). These data were combined to create maps that summarize structural analysis, slope, geothermometry, and heat. We also mapped discharge areas (to constrain elevations where groundwater may be discharged through modern thermal springs or paleo-thermal springs). We also mapped subcrops, which are possible erosionally- or structurally-controlled breaches in regional-scale aquitards that form the basis of our hydrogeologic windows concept. These two maps were particularly useful in identifying known geothermal systems and narrowing the search for unknown geothermal prospects. We further refined the "prospectivity" of a geothermal resource in the regions within the subcrops and discharge areas by developing and applying a new method for spatial association analysis to data on known and inferred faults, earthquakes, geochemical thermometers, and heat flow. This new methodology determines the relationships of the location and magnitudes of observations of these data with known geothermal sites. The mean prospectivity value for all regions with positive prospectivity was 1.83 (standard deviation = 0.75), whereas this mean prospectivity for known geothermal sites was 3.07 (standard deviation = 0.90). The prospectivity approach also substantially decreases the search area and increases the number of known geothermal resources per km^2 (from 0.004 at prospectivity > 0 to 0.016 at prospectivity > 3), suggesting that limiting an exploration area to regions with high prospectivity scores could reduce exploration costs. These results suggest that the prospectivity analysis using our integrated framework and the hydrogeologic windows concept is useful for identifying known and potential geothermal resources.

1. INTRODUCTION

Geothermal energy can technically be employed anywhere on Earth, and in the United States there is the potential for at least 280,000 exajoules (roughly 2,700 times annual U.S. energy consumption) of retrievable geothermal energy (Tester et al. 2006; U.S. Energy Information Administration 2015). But the opacity of the earth limits the ability to find and use geothermal resources, many of which are blind and do not have classic indications of a geothermal resource at the surface (e.g., hot springs, fumaroles, sinters, travertine deposits, argillic alterations, and propylitic alterations (Owens 2013)). The concept of Hydrogeologic Windows—areas of discharge or recharge through a breached aquitard with substantial vertical groundwater flow—can be applied to organize numerous data that are necessary, but individually insufficient, to identify a blind geothermal resource. Geothermal resources have three characteristics: (1) a heat source, (2) a permeable path to and from that heat source, and (3) a sufficient amount of fluid to extract and carry heat to accessible depths.

1. The amount of heat available at a certain depths can vary considerably. The type of rock present in any given portion of the subsurface is the primary determinant of how much heat can be mined, and how quickly the heat will regenerate.
2. Highly permeable regions are necessary to allow fluid flow to and from the heat source. Although these permeable regions may be apparent at the surface, it may be difficult to determine where these permeable regions exist in the subsurface.
3. Local, subregional, or regional groundwater systems can provide fluids in sufficient volume to commercially develop advective systems associated with hydrogeologic windows (Förster & Merriam 1999).

2. METHODS: INTEGRATED FRAMEWORK AND SPATIAL ASSOCIATION

We developed an integrated framework for locating hydrogeologic windows that combines multiple data sources and analyses and we applied this framework to a case study in southwestern New Mexico (Figure 1). Each method in the framework contributes information about the presence of least one of the physical features of a geothermal resource as indicated by the colored boxes for each data type or analysis. We used the outcomes of these analyses to estimate the "prospectivity" of an area, which indicates the relative likelihood of a

geothermal resource being present in that area. We chose to estimate "prospectivity" rather than "risk", because risk is defined as the product of the probability and magnitude of an outcome; analyses that estimate probabilities and magnitudes are difficult to properly constrain in approaches that attempt to identify blind geothermal resources. We developed an approach to spatial association analysis that we applied to a subset of the primary and secondary data in the integrated framework. We describe this spatial association analysis next, and then present more details on analyses within the integrated framework.

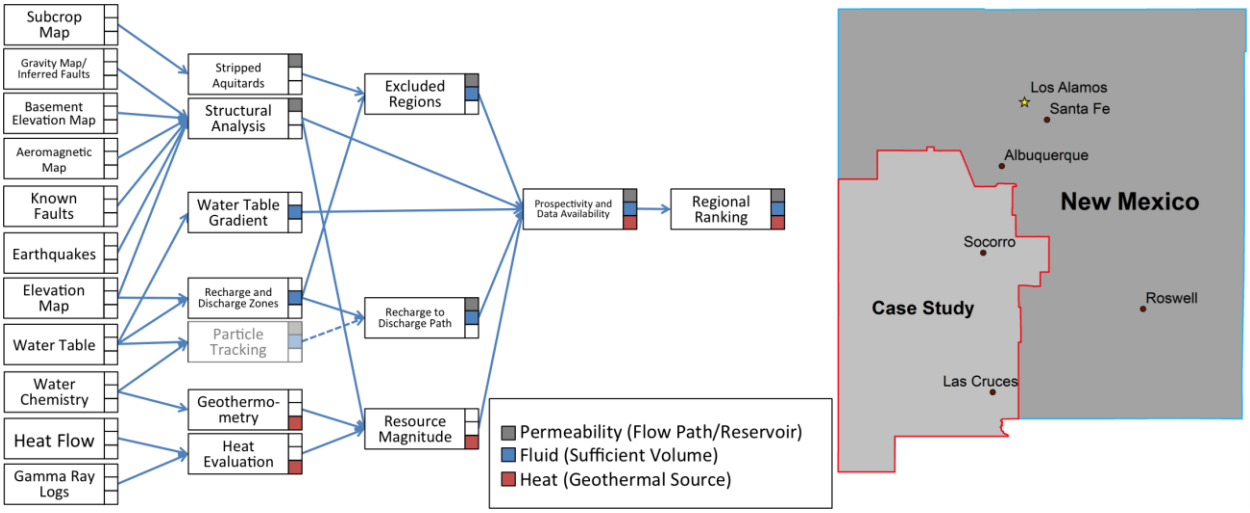

Figure 1: The integrated framework for identifying blind geothermal prospects using the hydrogeologic windows concept. The left-most column lists the data that were used for this study. Particle tracking has been described elsewhere and is not included in the analysis here (Person et al. 2015).

2.1 Spatial Association Analysis

Our spatial association analysis method is based on the cross-K function, also referred to as the bivariate, multivariate, or multi-type K function (Dixon et al. 2002). This method improves upon previous approaches that identify the spatial association of geothermal resources (e.g., Carranza et al. 2008). Our method is designed around the idea that if one were to assume that the data in the study region is randomly distributed, then the intensity, λ, is uniform across the region A and scales linearly with the number of points in the region. Intensity (λ) is defined as the number of events expected per unit area. A spatial point process is the stochastic process through which values are assigned to an event in space. Under a random distribution (a homogeneous Poisson process), the intensity of the region A should be $\hat{\lambda} = \frac{N}{|A|}$, where N is the number of events in the region, and $|A|$ is the area of the region.

If the spatial point process that is responsible for assigning values to these points is also a random process, points can be removed based upon these assigned values and will be equivalent to removing the points at random. Removing points at random will lower the intensity, but λ will remain constant throughout the region A. If the values are not randomly assigned, but instead reflect some underlying spatial distribution, then the intensity will vary within A based upon the spatial point process responsible for generating these values. For example, if the values are a function of the distance from geothermal locations, the intensity around geothermal locations will be higher than in the rest of the study area. The cross-K function describes the expectation for randomly distributed events i with intensity λ_i within a distance h of events in j:

$$K_{ij}(h) = \frac{E[\text{number of events in } i \text{ within } h \text{ of a randomly chosen event in } j]}{\lambda_i} \quad (1)$$

The conceptual outcome of this function is the area within which we would expect to see the given number of points at the given intensity. Under a random distribution of points the value of the cross-K function should be $\approx \pi h^2$. When edge effects are corrected for, this function can be estimated by:

$$\hat{K}_{ij}(h) = \frac{\sum_k \sum_l w(i_k, j_l) \times d(d(i_k, j_l) < h)}{\hat{\lambda}_i \hat{\lambda}_j |A|} \quad (2)$$

where $\widehat{\lambda_i}$ is the intensity of the events in i, $\widehat{\lambda_j}$ is the intensity of the events in j, A is the area of the study region, $d(i_k, j_l)$ is the distance between events i_k and j_l, $\delta(d(i_k, j_l) < h) = \begin{cases} 1 & d(i_k, j_l) < h \\ 0 & d(i_k, j_l) \geq h \end{cases}$, and $w(i_k, j_l)$ is the ratio of the area inside the boundary to the total area (Dixon et al. 2002). We can compare the deviation from randomness by using $\hat{L}$, where $\hat{L}(h) = \sqrt{\frac{\hat{K}_{ij}(h)}{\pi}}$. The conceptual outcome of this function is the radius that will sweep out the necessary area as defined by the cross-K function. So if the data were generated randomly, $\hat{L}(h) - h \approx 0 \; \forall h$, where any variance from zero is due to the discrete nature of the realization of the homogeneous Poisson process. The plotting of $\hat{L} - h$ is referred to as the $\hat{L}$ plot (Waller & Gotway 2004). Holding the intensities, $\widehat{\lambda_i}$ and $\widehat{\lambda_j}$, constant, and varying h, the expected mean of $L - h$ will remain $= 0$, while the value of $\hat{L} - h$ should vary, thus revealing the degree of spatial association at the distance h.

Spatial association as described by $\hat{L} - h$ can technically be positive or negative, but we only used positive spatial association. In order for each geothermal signature to have equal weight in the final prospectivity map, each of the spatial association graphs are normalized by dividing each spatial association value by the sum of spatial association for that signature. Hence the lithium concentration may have more spatial association than boron concentration, but each will only contribute a maximum of 1 to the prospectivity score of any region.

The spatial association for a type of data was estimated for the values at least as high as the value of the observation. The resulting spatial association graphs were 3-dimensional graphs providing a spatial association curve across distance for every threshold (top right corner of Figure 2). Our analysis indicated that there was little spatial association for Li concentrations below 1.315 mg/L and for B concentrations below 0.839 mg/L, so we only included the results of the spatial association above those concentrations. Our spatial association analysis of earthquake magnitudes did not yield a threshold, so we included the spatial association over the full range of observations. In addition, a threshold does not apply for known faults and inferred faults, because they either exist or they do not, so we used the spatial association for the full range of data.

To minimize distance warping during the mapping process, the coordinates of each observation were converted into azimuthal-equidistant coordinates with the azimuth being the center of all observations of that type. The spatial association curve matching the chosen threshold was then added onto that observation location in a 360° rotation, creating a "ripple" that originates from each observation. These ripples were summed together and the map was normalized by dividing each raster cell value by the maximum value for that observation type.

2.2 Mapping and Related Analyses

Stripped Aquitards

Aquitards restrict the flow of water in the subsurface. The subcrop map shows regions where aquitards have been tectonically/erosionally stripped or breached (i.e. hydrogeologic windows). Regions in which aquitards are present are unlikely to contain advective geothermal system, and thus the Subcrop map is used as an exclusionary layer in the integrated framework.

Structural Analysis

Our structural analysis used the following data: earthquakes, known faults, gravity, aeromagnetic, topographic elevation, oil/water wells, formation tops, and thermal wells/springs. The structural analysis (a) identified possible faults using the gradient of the gravity data, (b) estimated the spatial association of these inferred faults, known faults, and earthquakes with known geothermal resources, and (c) estimated the depth to Proterozoic basement.

Water Table Gradient

The water table gradient elicits regions with rapid rises and falls in the water table, indicating the possibility of 'substantial vertical groundwater flow' as required by the definition of hydrogeologic windows. An early water table map was acquired from the New Mexico Office of the State Engineer. We revised this map by incorporating estimates of where the first measurements at each location reflect the natural level of the water table prior to development and human withdrawal of groundwater. We used this "natural" water table in order to elicit a better picture of regions where the elevation of the water table naturally increases or decreases rapidly.

Recharge and Discharge Zones

Recharge zones are areas where precipitation may permeate into the subsurface, whereas discharge zones are areas the water table could reach or go above topographic elevation. Areas within a discharge zone are considered to have sufficient fluid volume for the existence of a geothermal resource. Water may not be present at the surface within a discharge zone because it could be impeded by local-scale geologic formations forming aquitards.

Geothermometry

The spatial association of geochemical tracers and geothermometers (Li, B) are included in the prospectivity because observations of elevated concentrations of these elements are known to be associated with geothermal resources (Sánchez-Alfaro et al. 2015; Fournier 1977; Owens 2013).

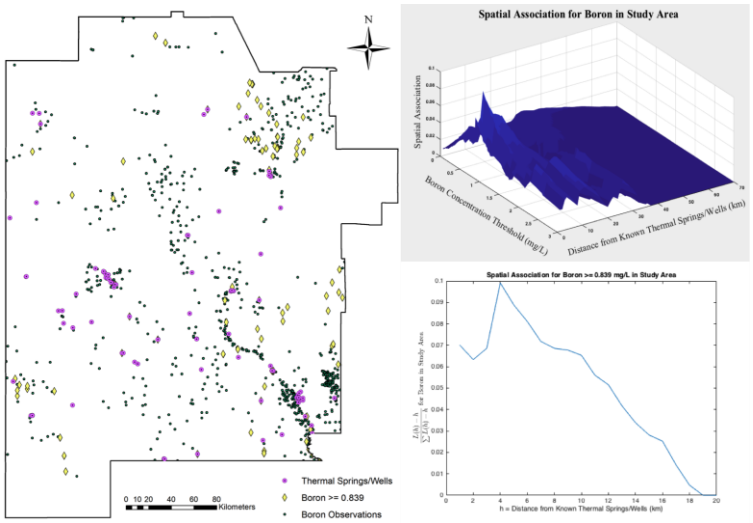

Figure 2. Boron observations in the study area, the 3-D spatial association graph, and the spatial association curve applied to observations above 0.839 mg/L.

Heat Evaluation

Heat flow is also often used as an indicator of geothermal resources (Owens 2013). Heat flow data for the state of New Mexico were compiled as part of the National Geothermal Database System (NGDS) effort. These data largely come from two sources: (1) published data from wells >200 m deep (e.g. Reiter et al. 1975) that measure the regional scale back-ground heat flow, and (2) industry data (AMAX, Hunt, etc.) from wells < 200 m deep that measure heat transfer in more localized hydrogeologic systems. These data were used to calculate the geothermal gradient, and then multiplied by the difference between surface elevation and basement elevation. The surface temperature was then added to the map to create a basement temperature map. The surface temperature was determined by the equation:

$$T_S(°C) = -7.22 \times 10^{-3} \times \text{elevation (m)} + 25.13 \quad (3)$$

This equation was derived from 43 NOAA climate stations in southwestern New Mexico. This basement temperature map provides a measure of the maximum amount of heat that could be extracted from a location.

2.3 Prospectivity

The prospectivity value for a location was calculated by:

$$\text{Prospectivity} = [HF + BT + KF + IF + Li + B + Eq + \nabla WT] \cdot SC \cdot DZ \quad (4)$$

where HF = heat flow, BT = basement temperature, KF = known faults, IF = inferred faults, Li = lithium, B = boron, Eq = earthquakes, ∇WT = water table gradient, SC = subcrop, and DZ = discharge zones. In terms of the three necessary characteristics of a geothermal resource, these signatures provide information on the presence of heat (HF, Li, B, BT), permeability (KF, IF, Eq, SC), and fluid (∇WT, DZ). The values for each of the signatures were weighted equally and were scaled between 0 and 1 so that, aside from the exclusionary signatures, each signature contributed at most the same amount to the overall prospectivity calculation. The prospectivity map is shown in Figure 3A.

2.4 Data Availability

The amount, location, and types of data that are available will limit the predictive capability of this analysis. The prospectivity map, when used in conjunction with the data availability map (Figure 3B), identifies the degree to which locations may contain geothermal resources, as well as the confidence that can be placed in that assessment. The data availability map was created using equal weighting for each data type, and summing together data density maps for each observation type (heat flow, basement temperature, lithium, boron, water table).

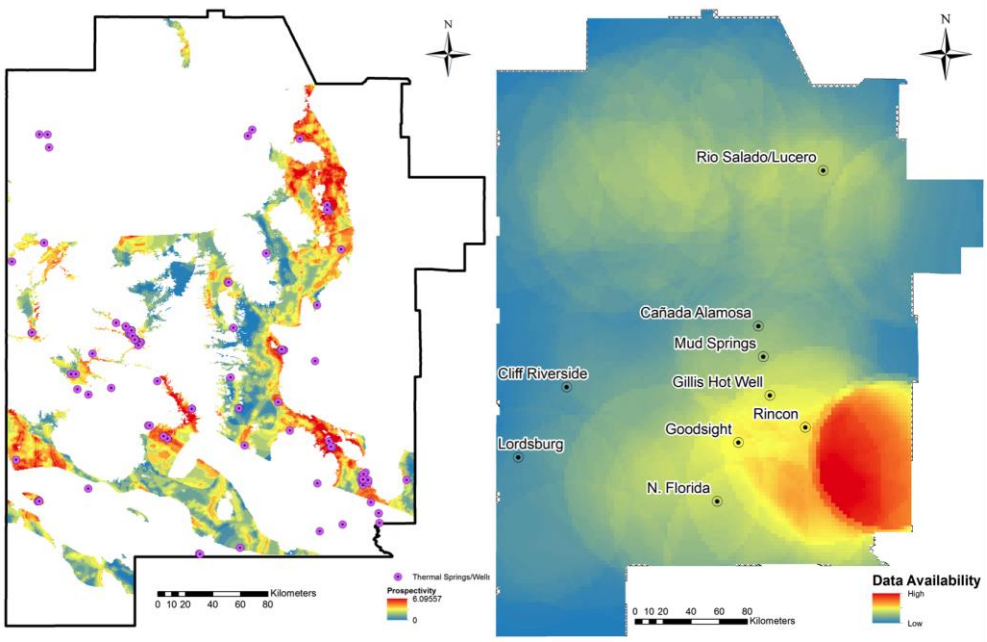

Figure 3. A. The prospectivity map with known thermal springs/wells; B. The data availability map with locations of future data collection indicated.

3. PROSPECTIVITY COMPARISON

3.1 Heat Flow

Heat flow (Figure 4) provides a point of departure for assessing areas for their potential to contain a blind geothermal resource. Areas with heat flow above 100 mW/m^2 may be considered areas with high heat flow and could thus be used as an initial screen for a geothermal resource. Table 1 summarizes the number of thermal wells and springs in the heat flow map in Figure 4. The table shows that heat flow with a threshold of 100 mW/m^2 locates about half (62/115) of the known thermal wells and springs. But the area in which the heat flow is above 100+ mW/m^2 is 24,338 km^2. Further, a cluster of 23 known thermal wells and springs (roughly halfway between the northern and southern boundaries of the area, and roughly 1/3 to the east of the western boundary) is not in the area with high heat flow; these known geothermal sites are in the area where the heat flow is only 80-100 mW/m^2. This is partly due to the lack of measurements of heat flow in the area, and thus the interpolated heat flow in this area is not controlled by nearby observations.

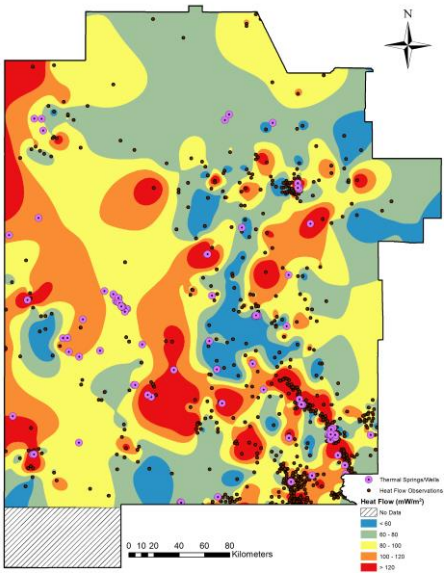

Figure 4. Interpolated heat flow with the locations of thermal springs/wells and heat flow observations.

Table 1 shows the number of known geothermal locations areas with different levels of heat flow. There are 53 thermal wells and springs in areas where the heat flow is less than 100 mW/m^2, but twenty of those 53 known geothermal sites are in areas with positive

prospectivity if heat flow is not considered in the prospectivity calculation. In contrast, there are 47 thermal springs and wells that exist in regions with a prospectivity value of 0, of which only fourteen are inside the regions with heat flow greater than 100 mW/m^2.

Table 1. Breakdown of geothermal sites by heat flow.

Heat Flow (mW/m^2)	*Geothermal Sites in Area*	*Area (km^2)*	*Density (geothermal sites/km^2)*
60+	106	86,968	0.001
80+	99	58,130	0.002
100+	62	24,338	0.003
120+	52	7,867	0.007

Our prospectivity map identifies known geothermal sites with better resolution than heat flow alone. For example, there is a thin line with positive prospectivity in Figure 3A that traces the same arc as the aforementioned cluster of thermal wells and springs (average prospectivity for these geothermal sites is 3.2, max is 4.0). Further, the prospectivity map substantially reduces the area to consider. Table 2 shows a summary of the prospectivity map. Table 2 shows that 62 known geothermal sites are located in areas with a prospectivity value greater than 2, which equals the number that are identified in the region with high heat flow (100+ mW/m^2) in Table 1. The area with prospectivity greater than two is also much smaller than the area with high heat flow: 7,906 km^2 vs. 24,338 km^2. The density of the number of thermal wells and springs that are located per unit of area is 0.008 for the prospectivity map, and more than 2.5x the density in the heat flow map (0.003). For higher heat flow (120+ mW/m^2), 52 known geothermal sites are in an area of 7,867 km^2, whereas 42 are identified in a much smaller area (2,702 km^2) with prospectivity greater than 3, and the density is more than twice as much.

Table 2. Characteristics of How Our Prospectivity Map Identifies Known Thermal Springs/Wells (Geothermal Sites) within Our Case Study in New Mexico - the left side of the table is based on the prospectivity values, and the right side is based on the quintile in which the prospectivity value falls.

Prospectivity Value	*Geothermal Sites*	*Area (km^2)*	*Density*	*Quintile (Prospectivity Value)*	*Geothermal Sites*	*Area (km^2)*	*Density*
>0	68	18,375	0.004	>0% (0.00)	68	18,375	0.004
>1	65	14,547	0.004	>20% (0.96)	65	14,697	0.004
>2	62	7,906	0.008	>40% (1.46)	64	11,009	0.006
>3	42	2,702	0.016	>60% (2.06)	61	7,338	0.008
>4	6	454	0.013	>80% (2.73)	52	3,654	0.014

The right side of Table 2 summarizes the prospectivity map by quintiles, in order to characterize the efficacy of the prospectivity map in a way that considers the imperfect and incomplete data. The prospectivity value corresponding to each quintile is indicated in parentheses under the percentage of the quintile. The quintiles reinforce the depiction of the distribution of prospectivity values by area in Figure 5. For example, 80% of the area with positive prospectivity in the prospectivity map has a prospectivity value of 2.73 or less. There are 52 known geothermal sites located in the 3,654 km^2 that have prospectivity values in the top 20% (i.e., > 2.73).

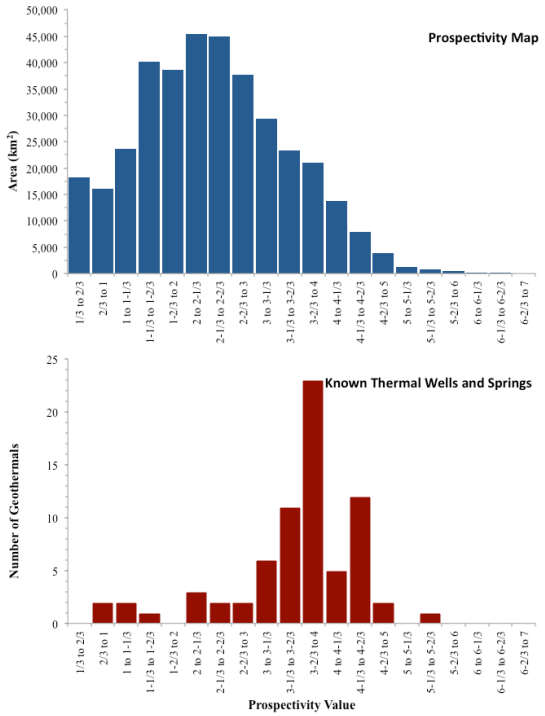

Figure 5. Distribution of the values of the prospectivity map (top) and the prospectivity values for known thermal springs/wells (bottom).

4. CONCLUSION

The analyses conducted in this project helped to provide information on three necessary characteristics for geothermal resources: permeability, fluid, and heat. By combining these analyses in our framework (Figure 1), we estimated the prospectivity that a location may contain a blind geothermal resource. As prospectivity increases, the density (defined as known geothermal locations per unit of area) of those prospectivity values increases as well. The spatial association analysis method presented here helps to improve this density compared to a more standard presence-absence approach. The integration of all of the included layers was also shown to consistently increase the density for higher prospectivity values.

5. ACKNOWLEDGEMENTS

This research was funded by the U.S. Department of Energy, Geothermal Technologies Office, under grant DE-0841-1517.

6. REFERENCES

Carranza, E.J.M. et al., 2008. Spatial data analysis and integration for regional-scale geothermal potential mapping, West Java, Indonesia. *Geothermics*, 37(3), pp.267–299. Available at: http://linkinghub.elsevier.com/retrieve/pii/S0375650508000242 [Accessed July 12, 2014].

Dixon, P.M., El-Shaarawi, A.H. & Piegorsch, W.W., 2002. Ripley's K function. *Encyclopedia of Environmetrics*, 3, pp.1796–1803. Available at: http://www.biostat.umn.edu/~dipankar/pubh8472/RipleysK.pdf.

Förster, A. & Merriam, D.F., 1999. *Geothermics in Basin Analysis*, New York: Kluwer Academic / Plenum Publishers.

Fournier, R., 1977. Chemical geothermometers and mixing models for geothermal systems. *Geothermics*, 5(1970), pp.41–50. Available at: http://www.sciencedirect.com/science/article/pii/0375650577900074 [Accessed December 4, 2014].

Owens, L., 2013. *Geochemical Investigation of Hydrothermal and Volcanic Systems in Iceland, New Mexico and Antarctica.* New Mexico Institute of Mining & Technology. Available at: http://www.ees.nmt.edu/outside/alumni/papers/2013d_owens_lb.pdf [Accessed December 4, 2014].

Person, M. et al., 2015. Hydrogeologic Windows : Detection of Blind and Traditional Geothermal Play Fairways in Southwestern New Mexico Using Conservative Element Concentrations and Advective-Diffusive Solute Transport. In *GRC Transactions*. pp. 751–759.

Reiter, M. et al., 1975. Terrestrial heat flow along the Rio Grande rift, New Mexico and southern Colorado. *Geological Society of America Bulletin*, 86, pp.811–818.

Sánchez-Alfaro, P. et al., 2015. Crustal deformation effects on the chemical evolution of geothermal systems: the intra-arc Liquiñe–Ofqui fault system, Southern Andes. *International Geology Review*, 55(April), pp.1384–1400.

Tester, J.W. et al., 2006. *The Future of Geothermal Energy:Impact of Enhanced Geothermal Systems (EGS) on the United States in the 21st Century*, Available at: https://mitei.mit.edu/system/files/geothermal-energy-full.pdf.

U.S. Energy Information Administration, 2015. *Electric Power Monthly: with data for May 2014*, Washington, DC.

Waller, L.A. & Gotway, C.A., 2004. *Applied Spatial Statistics for Public Health Data*, Hoboken, N.J.: John Wiley & Sons.